



**HAL**  
open science

## **Spatial variability and sources of platinum in a contaminated harbor – tracing coastal urban inputs**

Melina Abdou, Jörg Schäfer, Teba Gil-Díaz, Mary-Lou Tercier-Waeber, Charlotte Catrouillet, Francesco Massa, Michela Castellano, Emanuele Magi, Paolo Povero, Gérard Blanc

### ► To cite this version:

Melina Abdou, Jörg Schäfer, Teba Gil-Díaz, Mary-Lou Tercier-Waeber, Charlotte Catrouillet, et al.. Spatial variability and sources of platinum in a contaminated harbor – tracing coastal urban inputs. *Environmental Chemistry*, 2019, 17 (2), pp.105-117. 10.1071/EN19160 . hal-03637370

**HAL Id: hal-03637370**

**<https://hal.science/hal-03637370>**

Submitted on 11 Apr 2022

**HAL** is a multi-disciplinary open access archive for the deposit and dissemination of scientific research documents, whether they are published or not. The documents may come from teaching and research institutions in France or abroad, or from public or private research centers.

L'archive ouverte pluridisciplinaire **HAL**, est destinée au dépôt et à la diffusion de documents scientifiques de niveau recherche, publiés ou non, émanant des établissements d'enseignement et de recherche français ou étrangers, des laboratoires publics ou privés.



20 **Abstract**

21 Biogeochemical cycles including processes controlling platinum (Pt) distribution remain  
22 widely unknown in aquatic environments, especially in coastal systems. Dissolved Pt  
23 concentrations in coastal seawater ( $Pt_D$ ) and in Suspended Particulate Matter (SPM,  $Pt_P$ ) were  
24 measured, together with master variables comprising dissolved oxygen, dissolved and  
25 particulate organic carbon, chlorophyll-a, turbidity, and ammonium levels, along two  
26 longitudinal profiles in the industrial Genoa Harbor (northwest Italy). Concentrations and  
27 spatial distribution of  $Pt_D$  and  $Pt_P$  levels reflect distinct concentration gradients that were  
28 attributed to different Pt sources such as hospital, domestic and industrial wastewater,  
29 atmospheric deposition, and/or road run-off. Concentrations reaching up to  $0.18 \text{ ng.L}^{-1} Pt_D$  and  
30  $14 \text{ ng.g}^{-1} Pt_P$  reflect the impact of Pt urban inputs in coastal sites. These first data highlight  
31 considerable anthropogenic contamination in the confined harbor compared to the proposed  
32 reference value for the western Mediterranean surface seawater measured at external sites.  
33 Identified correlations between Pt levels and human pollution signals suggest the potential use  
34 of Pt as a new tracer of anthropogenic inputs that can be applied in other urbanized coastal  
35 systems. Biogeochemical processes inducing changes in partitioning and fate of Pt in coastal  
36 seawater reflect spatial variability, highlighting the need for comprehensive environmental  
37 monitoring at appropriate spatial scale.

38 **Keywords:** Platinum; Technology Critical Element; emerging contaminant; seawater;  
39 suspended particulate matter; distribution coefficient; urban tracer; coastal environment

40

## 41 **1. Introduction**

42 Platinum (Pt) is a Technology Critical Element (TCE) and an emerging contaminant of growing  
43 concern according to evidences of anthropogenic disturbance on its global biogeochemical  
44 cycle (Rudnick and Gao, 2003; Cobelo-García et al., 2015). Among its specific properties, Pt  
45 is an excellent catalyst used in industrial processes, such as petroleum chemistry, but more  
46 importantly in vehicle catalytic converters to reduce gaseous pollutants in exhaust fumes.  
47 Strongly increasing Pt demand for this technology results in growing anthropogenic Pt inputs  
48 into the environment, leading to a global increase of Pt concentrations in all environmental  
49 compartments including soils, atmosphere and aquatic systems (e.g. Rauch et al., 2006; Rauch  
50 and Morrison, 1999; Schäfer et al., 1999). However, other anthropogenic Pt sources (potentially  
51 implying the release of different Pt species to the environment) may occur in aquatic  
52 environments including Pt-derived anti-cancer drugs (e.g. Vyas et al., 2014).

53 Coastal areas are facing high anthropogenic pressure due to the increasing density of human  
54 population in such attractive zones (Small and Nicholls, 2003). Monitoring of trace metal  
55 concentrations in these sites is therefore essential to detect potential contamination and prevent  
56 associated adverse consequences on the ecosystem, especially for emerging contaminants.  
57 Platinum concentration in seawater is difficult to quantify precisely, in particular in less  
58 contaminated sites, because of extremely low environmental levels (sub  $\text{ng.L}^{-1}$ ; Mashio et al.,  
59 2017). Existing studies on marine coastal areas, including saline estuaries, report dissolved Pt  
60 concentrations ranging from 0.05 to 0.30  $\text{ng.L}^{-1}$  (Cobelo-García et al., 2013, 2014a; Goldberg  
61 et al., 1986; Mashio et al., 2016, 2017; Obata et al., 2006; Turetta et al., 2003; van den Berg  
62 and Jacinto, 1988). A small number of studies report Pt concentrations in Suspended Particulate  
63 Matter (SPM) ranging from  $\sim 2$  to 10  $\text{ng.g}^{-1}$  in the Lérez Estuary and from  $\sim 0.2$  to 1  $\text{ng.g}^{-1}$  in  
64 the Gironde Estuary (Cobelo-García et al., 2013, 2014a). Variations in Pt concentrations and

65 possible Pt enrichment in those coastal sites have been attributed to Pt inputs from human  
66 activities, especially in systems receiving anthropogenically-impacted freshwater inputs, as observed in the Tokyo Bay (e.g. Obata et al., 2006). Several studies  
67 have addressed bioaccumulation of Pt in wild marine bivalves, such as oysters and mussels  
68 (Abdou et al., 2016; Neira et al., 2015). However, there is a lack of data on the comprehensive  
69 characterization of the factors controlling the behavior of Pt in coastal seawater, including its  
70 partitioning between suspended particles and seawater, and huge uncertainties remain  
71 concerning its transport, bioavailability and fate in the coastal ocean (Cobelo-García et al.,  
72 2013).

74 The Mediterranean Sea is a semi-enclosed system under ever-growing anthropogenic pressure  
75 along its northwestern coast, comprising several highly populated cities with extensively  
76 urbanized and industrialized areas (Martín et al., 2009). Considering the possible changes in  
77 seawater chemistry due to additional anthropogenic inputs, previous studies have addressed  
78 environmental quality in historical and industrial harbors such as the Toulon Bay or the Genoa  
79 Harbor, reflecting intense pollution by metals, (e.g. Oursel et al., 2013; Tessier et al., 2011),  
80 metal-organic components (Pouget et al., 2014) and nutrients (Ruggieri et al., 2011). The  
81 Genoa Harbor on the northwest coast of Italy (Ligurian Sea) is one of the most important ports  
82 of the Mediterranean Sea, known for heavy contamination due to a variety of human activities.  
83 For many years, industrial effluents were the major cause of water pollution in this site, before  
84 the closure of the main heavy industries adjacent to the harbor during the 1990s. Nowadays,  
85 discharges from sewage treatment plants and from creeks account for generally high levels of  
86 nutrients, organic matter and faecal pollution in the harbor waters (Ruggieri et al., 2011).

87 The present work provides first information on Pt levels and spatial distribution in this major  
88 Mediterranean harbor combined with physical-chemical parameters. Such findings may help to

89 improve our understanding on Pt sources, other than the commonly assumed influence from  
90 catalytic converter emissions, and Pt cycling in an anthropogenically impacted coastal site. The  
91 objectives are therefore: (i) to quantify Pt levels and spatial distribution in a marine system  
92 under strong anthropogenic influence, involving different Pt sources, (ii) to characterize the  
93 factors controlling Pt distribution and partitioning between seawater and suspended particles  
94 considered a prerequisite for a better understanding of its biogeochemical cycle in coastal  
95 environments, and (iii) to investigate the potential use of Pt as an innovative tracer of human  
96 inputs (traffic, wastewaters, industrial activities) in coastal environments.

97

## 98 **2. Experimental**

### 99 2.1. Study area and sampling strategy

#### 100 *The coastline of Genoa*

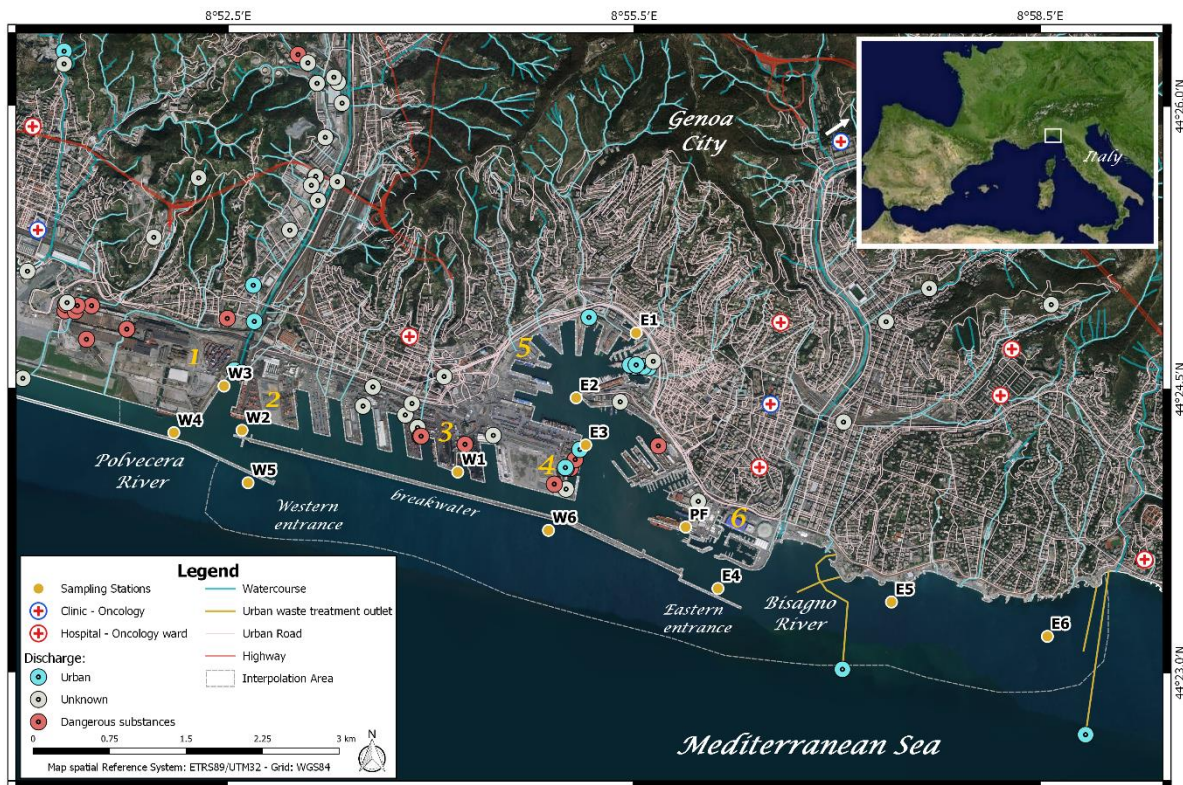
101 The Genoa Harbor is an artificial harbor on the northwest coast of Italy (44°24'39.8"N  
102 8°55'44.8"E). The port infrastructures extend over approximately 7 million m<sup>2</sup> along about  
103 20 km of coastline, protected by sea defenses and artificial breakwaters. The innermost, natural  
104 part of the Genoa Harbor is the so-called Old Port hosting a ferry terminal, several marinas and  
105 receiving urban treated sewage effluents (Ruggieri et al., 2011; Fig. 1). Outside the Old Port a  
106 wide, less confined area protected by artificial breakwaters extends to the east and to the west,  
107 hosting diverse industrial activities and receiving discharges from a coal-fired power plant,  
108 treated urban wastewater and untreated surface run-off (Ruggieri et al., 2011). In addition,  
109 important dredging has affected the area in the last decade (Cutroneo et al., 2012). Two  
110 seasonally active rivers discharge freshwater and treated wastewater into the harbor area: the  
111 Polcevera River to the west and the Bisagno River to the east (Fig. 1; catchment surface area of  
112 93 km<sup>2</sup> and 140 km<sup>2</sup>, respectively; Cutroneo et al., 2017)). Both rivers, characterized by

113 irregular and harsh streamflow fluctuations, run through the city of Genoa and are surrounded  
114 by dense urban structures hosting a variety of commercial and industrial activities.

### 115 *Sampling campaigns*

116 Two longitudinal profiles were performed to collect surface seawater and SPM samples inside  
117 and outside the Genoa Harbor on-board the Research Vessel MASO (3<sup>rd</sup> – 6<sup>th</sup> April 2017;  
118 Fig. 1). The first profile was carried out from the inner part of the port towards the eastern  
119 entrance (sampling sites E1 to E6; Fig. 1). This represents a supposed decreasing contamination  
120 gradient covering the strongly confined Old Port (sites E1 and E2), a less confined zone inside  
121 the breakwaters (site E3), the eastern Inlet (site E4) close to the mouth of the Bisagno River and  
122 two sites outside the Harbor, directly in contact with open Mediterranean water, i.e. the Ligurian  
123 Current (sites E5 and E6). This profile is performed along the less industrialized section of the  
124 harbor. The second profile addressed the western part of the Genoa Harbor (sampling sites W1  
125 to W6, Fig. 1) hosting coal deposits, a terminal for oil products (no storage tanks in the harbor),  
126 and receiving power plant discharges and inputs from the Polcevera River transporting sewage  
127 treatment plant effluents (Ruggieri et al., 2011).

128 Eastward profile was performed on April 3<sup>rd</sup> under north-northeast wind with an average speed  
129 of 16 km.h<sup>-1</sup> (Table 1; timeanddate.com). Westward profile was done the following day with  
130 weaker wind (~ 9 km.h<sup>-1</sup>) originating from south-southeast. Due to complex harbor shape,  
131 station bottom depth differs according to the location. Within the Old Port, site E1 has a bottom  
132 depth of 6 m (Table 1). Other sites within the breakwaters, show average depth of 11 m while  
133 it is of 16 m for E4 at the eastern inlet. We observe average depth of 14 m for external sites E5  
134 and E6, and 26 m for W5 and W6.



135  
 136 **Fig. 1:** Sampling sites in the Genoa Harbor. Two sampling profiles were performed with an  
 137 eastward profile (sites E1 to E6) and a westward profile (sites W1 to W6). Sampling site PF  
 138 (PlatForm) corresponds to the CNR Platform. Numbers correspond to main urban/industrial  
 139 activities with 1: Steel mill, 2: Bulk containers, 3: Coal power plant, 4: Oil storage, 5: Ferry  
 140 terminal, 6: Shipyards/marinas. Red crosses indicate hospitals with oncology ward with the  
 141 Oncology Clinics highlighted in blue. Colored circles show discharges from various sources.  
 142 Geospatial data provided by the Ligurian Administrative Region via own Geoportal - WFS  
 143 service (<https://geoportal.regiosne.liguria.it/>). Satellite image provided by ESRI©  
 144 (ArgGIS/Imagery)

145

146 Additional samples were taken at the CNR (National Research Council) Observation Platform  
 147 (site PF, Fig. 1) on April 6<sup>th</sup> 2017 at three different times of the day (10 am, 12 pm, 2 pm). The  
 148 bottom depth of this sampling site is of 6 m (Table 1). This sampling site is located at the limit  
 149 of the confined area of the harbor, supporting diverse harbor activities such as navigation, ship  
 150 construction and wrecking industries. Main hospitals with oncology ward of Genoa are located  
 151 rather close to this area, including an Oncology Clinic (~ 3 km).



152 *Sample collection*

153 Seawater and SPM samples were collected at all sites (i.e. on-board the R/V MASO or from  
154 the CNR Platform) by pumping surface water (~ 5 m depth) with a purpose-built low voltage  
155 (12 V) peristaltic pump connected to Teflon tubing. The latter was rinsed with seawater,  
156 accounting for more than three times the tubing volume (seawater pumping time of 10 min)  
157 prior to sample collection. Seawater was collected into acid-washed 500 mL Teflon bottles  
158 (Nalgene®), previously rinsed with pumped water at each site. Water samples for analyses of  
159 dissolved Pt ( $Pt_D$ ) were filtered immediately through 0.2  $\mu m$  polycarbonate filters  
160 (Nucleopore®) with a filter-syringe (Sartorius®) into acid-washed 60 mL Teflon bottles  
161 (Nalgene®), previously rinsed with an aliquot of the filtrate, then acidified to pH = 1 (36.5–  
162 38 % HCl Baker Instra) and stored in the dark at 4 °C pending analysis. Water aliquots from  
163 the 500 mL Teflon bottle were collected to quantify ammonium ( $NH_4^+$ ) and dissolved organic  
164 carbon (DOC) concentrations. The samples for  $NH_4^+$  analysis were filtered as aforementioned  
165 into pre-cleaned 15 mL polypropylene (PP) tubes (Kartell®), and stored frozen pending  
166 analysis. Aliquots for DOC were filtered through pre-combusted (500 °C, 4 h) glass-fiber filters  
167 (0.7  $\mu m$ , Whatman® GF/F) using a pre-cleaned (RBS detergent, thoroughly rinsed with ultra-  
168 pure deionised water, Milli-Q® water) and pre-combusted glass syringe. Filtrates were  
169 collected in pre-cleaned and pre-combusted glass bottles, acidified (HCl 0.3 % v/v; Baker,  
170 Analyzed) and then stored in the dark at 4 °C until analysis.

171 Particulate samples were collected for analyses of particulate platinum ( $Pt_P$ ) and particulate  
172 organic carbon (POC). In both cases, the sampling bottle was carefully shaken and seawater  
173 was placed in a pre-rinsed filtration unit covered by a lid. For  $Pt_P$ , SPM were collected on pre-  
174 weighed Teflon filters (47 mm, 0.45  $\mu m$  FHLC filter, Merck Millipore®), whereas for POC,  
175 SPM were collected on pre-combusted and pre-weighed glass-fiber filters (0.7  $\mu m$ , Whatman®  
176 GF/F). Once in the laboratory, both filters were then oven-dried (48 h at 50 °C) to constant

177 weight, re-weighed (to determine SPM content) and kept in the dark at room temperature  
178 pending analysis. A field blank was performed for all sampled parameters and processed in the  
179 same way as seawater samples but using Milli-Q water.

180

## 181 2.2. Analytical methods

### 182 *Platinum in seawater*

183 Seawater samples were analyzed by Adsorptive Cathodic Stripping Voltammetry (AdCSV) as  
184 described in Cobelo-García et al. (2014b). Measurements were carried out using a  $\mu$ Autolab  
185 Type III potentiostat (Metrohm®) connected to a polarographic stand (Metrohm® 663 VA  
186 Stand) equipped with three electrodes: (i) a hanging mercury drop electrode (HMDE, the  
187 working electrode), (ii) a silver/silver-chloride (Ag/AgCl) reference electrode, and (iii) a glassy  
188 carbon auxiliary electrode. A polytetrafluoroethylene (PTFE) voltammetric cell served in all  
189 experiments and the potentiostat was controlled using the NOVA 2.1® software. Elimination  
190 of organic matter by UV oxidation was performed by placing sample aliquots in capped Teflon  
191 bottles with overnight irradiation using two 64 W UV lamps (NIQ 60/35 XL, Heraeus) under a  
192 fume hood. Aliquots (10 mL) of UV-digested sample were pipetted into the voltammetric cell  
193 together with 30  $\mu$ L of 3.3 mM formaldehyde (37–41 % Analytical Reagent Grade, Fisher  
194 Chemical®), 30  $\mu$ L of 0.45 mM hydrazine sulfate (Analytical Reagent Grade, Fisher  
195 Chemical®), and 300  $\mu$ L of sulfuric acid (H<sub>2</sub>SO<sub>4</sub>, 93–98 % Trace metal grade, Fisher  
196 Chemical®). Platinum concentrations were quantified by standard internal addition method,  
197 adding a controlled amount of a Pt stock solution freshly prepared daily from a mono-  
198 elementary Pt standard solution (1000  $\mu$ g.mL<sup>-1</sup> PLASMACAL, SCP Science®). We applied a  
199 deposition time of 300 s and experimental parameters as described elsewhere (Cobelo-García  
200 et al., 2014b). In the absence of Certified Reference Material (CRM) for dissolved Pt in

201 seawater, analytical quality of the voltammetric procedure was evaluated by means of Pt spiked  
202 CRM seawater quantification (CASS-6, NRCC) giving recoveries > 80% and precision  
203 expressed as Relative Standard Deviation (RSD) lower than 10 % (n = 5) at the 0.5 ng.L<sup>-1</sup> range.  
204 The detection limit (D.L.) for dissolved Pt measured by AdCSV (calculated as 3 x blank  
205 standard deviation, n = 20) was estimated to 0.03 ng.L<sup>-1</sup>. Satisfactory results were obtained for  
206 field blank with Pt<sub>D</sub> of 0.05 ng.L<sup>-1</sup>.

207

### 208 *Platinum in SPM*

209 Particulate platinum concentrations (PtP) in Suspended Particulate Matter samples were  
210 analyzed by Triple Quadrupole-Inductively Coupled Plasma-Mass Spectrometry (TQ-ICP-MS,  
211 Thermo® iCAP TQ). Teflon filters with SPM (typical mass of ~ 3 - 5 mg) were acid digested  
212 as described in Abdou et al. (2018). Briefly, 2 mL HCl and 1 mL HNO<sub>3</sub> (30 % HCl and 65 %  
213 HNO<sub>3</sub> Suprapur, Merck®) were added to the samples in polypropylene (PP) tubes (DigiTUBEs,  
214 SCP SCIENCE®) and closed with caps. Samples were placed in a Teflon-coated heating block,  
215 and digested at 110 °C for 3 h. Cooled contents were then diluted in 10 mL Milli-Q water,  
216 centrifuged at 4000 rpm for 10 min (20 °C) and filters were discarded. Analyses were  
217 performed applying the standard internal addition method (as previously explained). After  
218 obtaining the raw signal, Hafnium-oxide (HfO<sup>+</sup>) interferences were monitored using the <sup>193</sup>Ir  
219 signal that is highly interfered by HfO<sup>+</sup> (Djingova et al., 2003). Raw signal was thereafter  
220 mathematically corrected using <sup>194</sup>Pt / <sup>195</sup>Pt natural ratio and assuming that HfO<sup>+</sup> is the  
221 only/dominant spectral interference on those selected isotopes. Analytical quality control was  
222 performed using the BCR®-723 road dust (Institute for Reference Materials and  
223 Measurements) and Jsd-2 sedimentary rocks (indicative value from Geological Survey of  
224 Japan) as available CRMs for Pt concentrations. Analyses of these CRMs by TQ-ICP-MS gave  
225 satisfactory recovery values of 87% and 101% respectively (n = 3) and precision expressed as

226 RSD of ~ 5 %. The detection limit (D.L.) for  $Pt_p$  ( $n = 10$ ) was estimated to  $0.34 \text{ ng.g}^{-1}$  for  
227 typical sediment sample mass of 4 mg. Satisfactory results were obtained for field blank with  
228  $Pt_p$  below detection limit.

229

### 230 *Complementary measurements*

231 Parallel to sampling, other master variables (i.e. temperature, dissolved oxygen, salinity, and  
232 turbidity) as well as chlorophyll-a (Chl-a) concentrations were measured *in situ* using a  
233 submersible probe (OS316*Plus*, Idronaut®), previously calibrated on-board the R/V MASO or  
234 in an on-site laboratory on the CNR Platform. Salinity was measured using the Practical Salinity  
235 Scale and Turbidity with Nephelometric Turbidity Units. Seawater pH and redox potential (Eh)  
236 were determined with a Sentix® 41 probe (PROFILINE, WTW) and a PH-25 probe  
237 (CRISON®), both previously calibrated using the manufacturer's specifications and supplied  
238 reagents (NIST pH standards).

239 Dissolved organic carbon (DOC) was analyzed with an automated analyzer (TOC-L,  
240 Shimadzu®) as described in Sharp et al. (1993). Accuracy of DOC measurements was tested  
241 using reference material (Deep Sea Reference, DSR, University of Miami) providing recovery  
242 results > 90 %. Analytical precision expressed as %RSD was 5 % at the  $0.5 \text{ mg.L}^{-1}$  range. The  
243 D.L. ( $n = 10$ ) was estimated to  $0.06 \text{ mg.L}^{-1}$ . Particulate organic carbon (POC) was analyzed  
244 with a LECO® CS-125 after carbonate elimination as described elsewhere (e.g. Schäfer et al.,  
245 2002). Analytical quality was checked by measuring CRMs (e.g. LECO 501–503). Accuracy  
246 was within 5 % of the certified values and the analytical error generally < 5 % (% RSD).  
247 Ammonium concentrations were determined by colorimetric procedure (visible-UV  
248 spectrophotometer, Thermo®, Genesys 20, Aminot et al., 1997). Analytical error of the method  
249 is < 5 % (% RSD), accuracy within 5 % of the reference values, and the D.L. of  $18 \text{ } \mu\text{g.L}^{-1}$ .

250 Satisfactory results were obtained for field blank values of DOC, POC and NH<sub>4</sub><sup>+</sup>  
251 (~ 0.2 mg.L<sup>-1</sup>, 0.04 %, and ~ 30 µg.L<sup>-1</sup> respectively).

252

### 253 2.3. Data treatment

254 The correlation matrix for the different parameters was produced using the software PAST®  
255 applying the linear r (Pearson) parametric correlation coefficient. The statistical significance  
256 (p-value) was set to 0.05. Surfer® software (Golden Software Inc., ver. 13) was used to produce  
257 the distribution maps of the analytical results and the data interpolation was performed using  
258 Minimum Curvature algorithm. Due to the complexity of the port area, a fault traces file of the  
259 port shape (Fig. 1) and a spatial resolution of 5 m were used to perform the calculation gridding.  
260 The interpolated variable limits were fixed to minimum/maximum of the measured data for the  
261 Pt<sub>D</sub> map; and from 0 until the maximum of the measured data for the Pt<sub>P</sub> map. For each  
262 interpolation map, the software returns the coefficient of multiple determination (R<sup>2</sup>), which  
263 represents the goodness of fit of the model. When the regression equation fits well to the data,  
264 R<sup>2</sup> is large and close to 1.

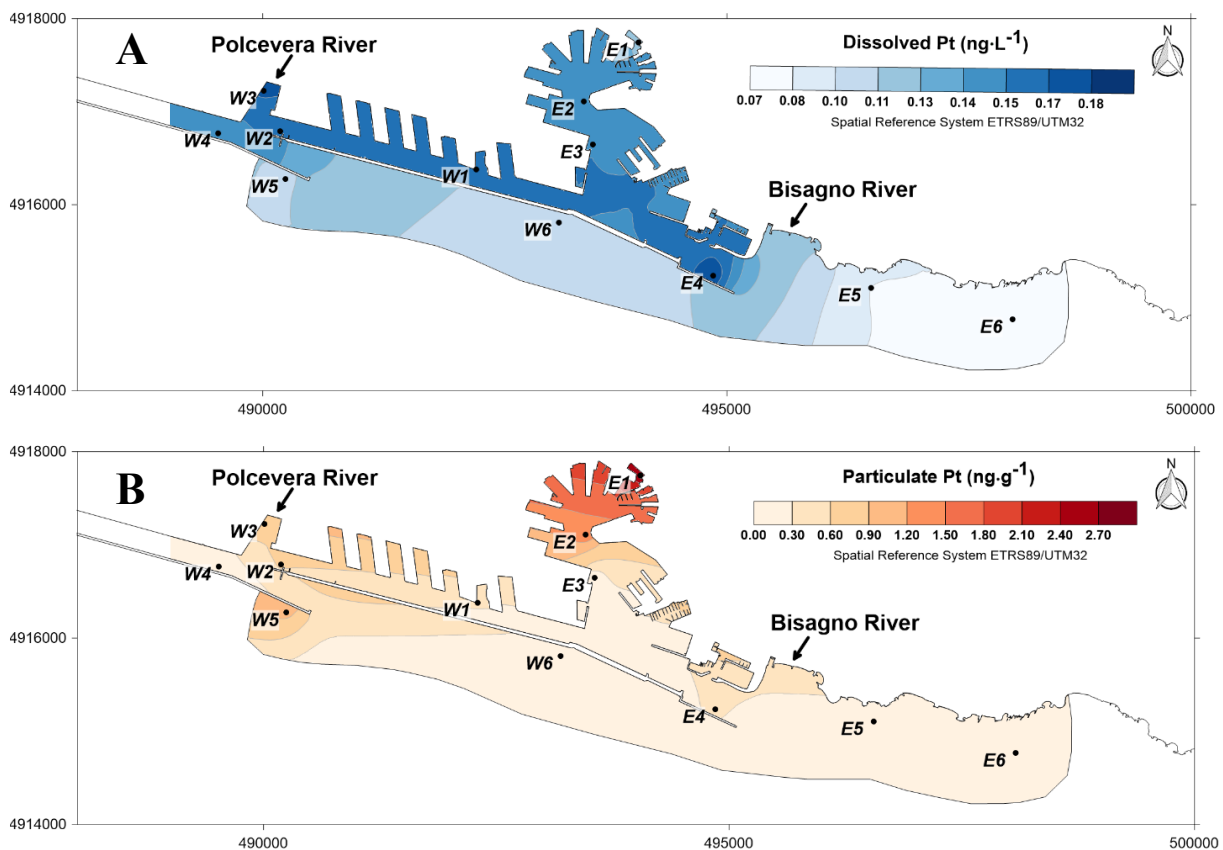
265 Particle–water distribution coefficients, K<sub>D</sub>, defining the concentration ratios of Pt<sub>P</sub> over Pt<sub>D</sub>  
266 were calculated according to the equation (1)

$$267 \quad K_D = [Pt_P] / [Pt_D] \times 10^3 \quad (1)$$

### 268 3. Results

269 The results obtained for major physical-chemical parameters and complementary  
270 measurements are represented for two distinct longitudinal profiles, both starting from inside  
271 the Genoa harbor and going towards the open Mediterranean Sea along the east and west part  
272 of the coastline (Table 1). A clear decreasing gradient occurred for turbidity values from inside  
273 towards the open sea eastward while westward profile featured no clear trend. Temperature  
274 values varied between 14.5 °C and 15.0 °C with a trend for higher temperature for sampling  
275 sites located inside the breakwaters. For both profiles, lowest temperatures occurred for external  
276 sites being E6 and W6. For the eastern profile, salinity (S) of ~ 37.7 in the inner harbor,  
277 compared to S = 38.0 in the outmost sites, suggested a ~ 1 % mixing of freshwater. Westward,  
278 only the site W1 showed lower salinity (37.8), whereas other sites showed average salinity of  
279 ~ 38. Redox potential (Eh) showed an increasing trend for eastward inner sites with highest  
280 value of 211 mV for site E4, while at external sites E5 and E6, lower values (~ 190 mV)  
281 occurred. Westward, Eh values did not show any particular trend (~ 180 mV), yet slightly  
282 higher values at external sites W5 and W6 (~ 204 mV). Measurements of pH varied between  
283 8.14 and 8.24, with highest values for external sites in both profiles (Table 1). Oxygen  
284 saturation levels, DOC, and POC ranged between ~ 70 % and 98 %; 0.7 and 2.0 mg.L<sup>-1</sup>; and  
285 1 % to 5 % respectively. An increasing gradient occurred for O<sub>2</sub> saturation eastward from inner  
286 to outer sites while levels of DOC, POC%, Chl-a and NH<sub>4</sub><sup>+</sup> decreased (except for one higher  
287 POC% value at site E5). Chlorophyll-a and NH<sub>4</sub><sup>+</sup> values at sites E5 and E6 were of  
288 ~ 0.3 µg.L<sup>-1</sup> and below the D.L. (18 µg.L<sup>-1</sup>), respectively. In contrast, the westward profile  
289 showed relatively constant values for O<sub>2</sub> saturation (~ 90 %). Elevated Chl-a, DOC, and POC %  
290 levels tended to occur for stations inside the breakwaters, while most NH<sub>4</sub><sup>+</sup> concentrations were  
291 below the D.L.

292 Dissolved Pt concentrations ranged from  $0.08 \text{ ng.L}^{-1}$  to  $0.18 \text{ ng.L}^{-1}$  (Table 1) and showed clear  
 293 concentration differences between sites inside the harbor and sites outside the breakwaters  
 294 (Fig. 2A). Despite the distance from the stations, a coefficient of multiple determination of 0.51  
 295 was obtained for  $P_{TD}$  map that clearly confirms the observed gradient (Fig. 2A). Westward  
 296 profile showed somewhat similar  $P_{TD}$  concentrations at the sites W1 to W3, all inside the  
 297 breakwaters, and a decrease towards the most distant site of this profile ( $\sim 0.10 \text{ ng.L}^{-1}$  at W6).  
 298 The eastward profile displayed an increasing  $P_{TD}$  gradient from  $\sim 0.10 \text{ ng.L}^{-1}$  at E1 to  
 299  $0.18 \text{ ng.L}^{-1}$  at E4 and a sharp drop towards lower values at sites E5 and E6 ( $0.08 \text{ ng.L}^{-1}$ ;  
 300 Table 1).



301  
 302 **Fig. 2:** Dissolved and particulate Pt concentrations along the two longitudinal profiles in the  
 303 Genoa Harbor. A: spatial distribution of dissolved Pt concentrations ( $P_{TD}$ ;  $\text{ng.L}^{-1}$ ); and B: spatial  
 304 distribution of particulate Pt concentrations ( $P_{TP}$ ;  $\text{ng.g}^{-1}$ ).

305 The observed  $Pt_P$  concentrations ranged from below D.L. ( $< 0.34 \text{ ng}\cdot\text{g}^{-1}$ ) up to  $\sim 3 \text{ ng}\cdot\text{g}^{-1}$   
306 (Table 1). A coefficient of multiple determination of 0.61 was obtained for the  $Pt_P$  map. Along  
307 the westward profile,  $Pt_P$  concentrations were relatively constant and low ( $< 1 \text{ ng}\cdot\text{g}^{-1}$ ; Fig. 2C)  
308 with values below D.L. in sites W4 and W6. In the eastward profile,  $Pt_P$  were highest in the Old  
309 Port (site E1), and showed an overall decreasing trend towards the outer sites reaching values  
310 below D.L. at sites E5 and E6 ( $Pt_P$  level at site E3 was also below the D.L.).

311 Calculated particle–water distribution coefficients varied from  $2 \times 10^3$  to  $23 \times 10^3$  and showed  
312 eastward and westward gradients similar to those observed for  $Pt_P$  concentration variations  
313 (Table 1).

314 The relationships between spatial variations of  $Pt_D$  and  $Pt_P$  concentrations and the other  
315 parameters measured are displayed separately for each profile only for the sites within the  
316 breakwaters (Table 2). Despite the low number of samples, results of the correlation matrix  
317 suggest that linear correlations exist between selected master variables and Pt levels in both the  
318 dissolved and particulate phases along the profiles (Table 2). Eastward,  $Pt_D$  concentrations  
319 seemed to be slightly positively correlated ( $r \sim 0.6$ ) with wind speed and pH, and significantly  
320 positively correlated ( $r > 0.9$ ) with Eh and  $O_2$ . These concentrations were significantly  
321 negatively correlated with turbidity, DOC, POC Chl-a, and with  $NH_4^+$  levels ( $r < -0.9$ ).  
322 Opposite behavior occurred for  $Pt_P$  concentrations. In the westward profile,  $Pt_D$  concentrations  
323 which were weakly positively correlated with turbidity, Eh, ( $r > 0.8$ ) and pH ( $r \sim 0.6$ ) and  
324 negatively correlated with  $O_2\%$  ( $r \sim -0.6$ ). Again  $Pt_P$  concentrations showed opposite behavior  
325 with significant correlations (Table 2).

326 Platinum concentrations at the CNR Platform (fixed site PF; Fig. 1) measured at three different  
327 times of the day showed variations for both  $Pt_D$  ( $0.09$  to  $0.15 \text{ ng}\cdot\text{L}^{-1}$ ) and  $Pt_P$  ( $3.1$  to  $14 \text{ ng}\cdot\text{g}^{-1}$ ;  
328 Table 3), with highest concentrations at 12 pm. Dissolved Pt concentrations were in the same



329 range as those measured along the profiles, whereas relatively higher  $P_{tP}$  levels occurred,  
330 leading to higher  $K_D$  values. During the measurements at the CNR Platform, wind direction  
331 changed from north to south with relatively weak wind speed, similar to those during the  
332 sampling of the westward profile. The master variables at the CNR Platform were in the same  
333 range as levels observed at other internal sites (Tables 1 and 3). Only dissolved  $O_2$  saturation  
334 values were somewhat lower than those measured along the longitudinal profiles and were close  
335 to those in the Old Port site (E1; Table 1). Dissolved Organic Carbon was also in the lower  
336 range compared to longitudinal profiles, with values similar to those observed at site E4.  
337 Ammonium values were close to those quantified during the westward profile.

338

## 339 **4. Discussion**

### 340 4.1. Water masses in the harbor and Pt distribution

341 Inside the harbor, water mass characteristics are supposedly strongly influenced by the  
342 wind/wave conditions, the freshwater supply by the two main water courses (the Polcevera and  
343 Bisagno Rivers), and run-off in the port area (Capello et al., 2010). Such physical parameters  
344 may influence Pt distribution in the Genoa Harbor. Cutroneo et al. (2012) report the formation  
345 of eddies in the current formed by wind in the Genoa area. The relative shallowness of the port  
346 area (Table 1) further accentuates the influence of the wind on the entire water column (Capello  
347 et al., 2010). Higher wind speed as recorded during the first day (Table 1) was correlated with  
348  $O_2$  saturation and turbidity ( $r \sim 0.8$  and  $-0.8$  respectively; data not shown). This result suggests  
349 an influence of wind speed on water mixing along the eastward profile. Along the westward  
350 profile, weaker winds (coming from the south and probably stopped by breakwaters) showed  
351 no correlation with  $O_2$  saturation levels. Considering only the eastward profile, increasing wind  
352 and subsequent water mixing is correlated with increasing  $P_{tD}$  and decreasing  $P_{tP}$  levels ( $r \sim 0.6$

353 and -0.9 respectively). In the inner harbor, strong wind could lead to vertical and horizontal  
354 seawater mixing, sediment resuspension, and redistribution of dissolved and especially  
355 particulate components throughout the water column as observed in other studies (e.g. El Sayed  
356 et al., 1994; see *Section 4.3.*).

357 The two profiles sampled westward and eastward from the Old Port show elevated  $Pt_D$   
358 concentrations within the whole harbor area, compared to the external sites (E5, E6 and W5,  
359 W6). The lowest  $Pt_D$  values occurred at the sites E5 and E6 (Fig. 2A) mainly influenced by  
360 open Mediterranean water transported with the east-west oriented northern Ligurian Current.  
361 Therefore, the  $Pt_D$  concentrations in seawater from these sites ( $\sim 0.08 \text{ ng.L}^{-1}$ ) may be considered  
362 as representative of surface water in the northwestern Mediterranean Sea. This assumption is  
363 supported by identical  $Pt_D$  levels of  $0.08 \text{ ng.L}^{-1}$  in surface waters from an open-sea site, south  
364 from the Balearic Islands (Abdou, 2018). Open Mediterranean surface water  $Pt_D$  concentrations  
365 appear somewhat higher than average  $Pt_D$  in the North Atlantic seawater reported in the early  
366 nineties ( $\sim 0.05 \text{ ng.L}^{-1}$ ; Colodner, 1991) and recently confirmed by López-Sánchez et al. (2019)  
367 for North, Central and South West Atlantic Ocean. Values are also higher than those reported  
368 in the northwest Pacific Ocean ( $\sim 0.04 \text{ ng.L}^{-1}$ ; Suzuki et al., 2014). However, the supposed  
369 Mediterranean surface water  $Pt_D$  is similar to values in the coastal North Atlantic Ocean off the  
370 slightly Pt-contaminated Gironde Estuary ( $0.08 \text{ ng.L}^{-1}$ ; Cobelo-García et al., 2014a) and lies  
371 within the range of values reported for the Lérez Estuary seawater end-member (from 0.08 to  
372  $0.10 \text{ g.L}^{-1}$ ; Cobelo-García et al., 2013). These observations are consistent with expected  
373 relatively higher Pt inputs into the semi-enclosed Mediterranean Sea due to the strong  
374 urbanization of its coastline. Similarly, the western profile shows the lowest  $Pt_D$  values (i.e.  
375  $\sim 0.10 \text{ ng.L}^{-1}$ ; Fig. 2A) at the sites located outside the breakwaters (W5 and W6). These  
376 concentrations are slightly higher than open Mediterranean  $Pt_D$ , suggesting minor local  
377 contamination off the harbor and ‘downstream’ from the sites E5 and E6 (with respect to the

378 dominant westward Ligurian Current). Conversely, inside the breakwaters, contamination is  
379 consistently higher with  $Pt_D$  concentrations up to more than 2-fold the open Mediterranean  
380 value (Fig. 2A).

381 Particulate Pt concentrations in suspended particles partly reflect the general concentration  
382 gradient from inside the harbor towards the open sea. They were measurable ( $\sim 0.4$  to  $3 \text{ ng.g}^{-1}$ )  
383 at all internal sites and behind the breakwaters (except site E3), whereas for the external sites  
384 from outside the breakwaters  $Pt_P$  were below D.L. ( $< 0.34 \text{ ng.g}^{-1}$ ; Fig. 2B). The  $Pt_P$  levels inside  
385 the Genoa Harbor were similar to those reported for the Lérez Estuary ( $\sim 1$  to  $15 \text{ ng.g}^{-1}$ ),  
386 interpreted as anthropogenic Pt enrichment (Cobelo-García et al., 2013). Such enrichment may  
387 partly originate from small watercourses flowing into the harbor (Fig. 1), even though salinity  
388 measurements show little influence of freshwater inputs. Since sampling took place at  $\sim 5 \text{ m}$   
389 depth i.e. below the main influence of freshwater torrents (Capello et al., 2016) and no strong  
390 rainfall occurred the previous days (only 3.8 mm on April 2<sup>nd</sup>), our salinity records mainly  
391 reflect seawater influence. In the inner part of the Old Port, the semi closed shape and shallow  
392 bottom ( $< 10 \text{ m}$  depth; Table 1) of the harbor make the water exchange times rather long, in  
393 particular close to the bottom depth (corresponding to E1 sampling point). Povero et al. (2005)  
394 calculated a mean of 20 days for a complete water exchange in this inner part and 7 days in the  
395 outer system (central basin and eastern entrance), which is wider and  $\sim 10 \text{ m}$  deeper. Although  
396 both calculated water residence times are not representative of the whole area (because they do  
397 not consider its irregular shape) and refer mainly to the eastward transect, they can help  
398 explaining the Pt enrichment in the inner part of the harbor. They may also explain the  
399 decreasing gradient towards the outer basin and the open sea, together with dilution affecting  
400 the generally stagnant harbor waters when flowing outside. Moreover, inside the harbor,  
401 important dredging activities were undertaken from 2009 to 2014 and are, to a lesser extent,  
402 still carried out in the recent years. Since then, turbid plumes, influenced by wind/wave

403 conditions, have been recorded (Cutroneo et al., 2012). Intensification of big ships and ferry  
404 transit and berthing increase the presence of turbid plumes (Capello et al., 2010), suggesting  
405 that sediment resuspension may represent a source of trace metals, including Pt, in the system.

406

## 407 4.2. Anthropogenic Pt sources

### 408 *Industrial activities*

409 Along the eastern profile, from the inner to the outer part of the harbor, Pt<sub>D</sub> concentrations  
410 tended to increase with a maximum at site E4, close to the mouth of the Bisagno River (Fig. 2A),  
411 while the highest Pt<sub>D</sub> in the westward profile occurred inside the breakwaters, including site  
412 W3 (0.17 ng.L<sup>-1</sup>), i.e. near the Polcevera River mouth. The western part of the harbor hosts coal  
413 deposits and a terminal for oil products (Fig. 1). Indeed, westward the Polcevera River mouth,  
414 the Multedo oil terminal is one of the most important in Italy and Europe. It handles crude oil,  
415 final products (petrol, gasoline, fuel oil) semi-manufactured, and basic petrochemical products,  
416 for a maximum total capacity of 30 million tons per year (Recchia et al., 1999). Platinum is  
417 commonly used as a catalytic agent in oil industry (e.g. catalytic cracking of crude petroleum;  
418 Peavy, 1958) and such activities could therefore be a source of Pt inputs into the coastal system.  
419 Built in 1952, the coal power plant of Genoa is also located on the west side of the harbor. Coal  
420 industry may contribute to local Pt concentrations, since high Pt concentrations have been  
421 reported for coal samples (~ 5 ng.g<sup>-1</sup>, Finkelman and Aruscavage, 1981; up to 70 ng.g<sup>-1</sup>, Dai et  
422 al., 2003). The bulk terminal of the harbor containing coal (dry bulk) and oil (liquid bulk) is  
423 also located in the western area (Cutroneo et al., 2017). Historical intense oil and coal-based  
424 industrial activities in the Genoa Harbor and erosion/leaching of such deposits stored uncovered  
425 against wind and/or rain might lead to the presence of industrial coal particles in the suspended  
426 particulate matter around the Polcevera River mouth and in the Sampierdarena channel that

427 connects the outer basin of the Old Port and Polcevera River mouth. Although the Pt  
428 concentrations in this oil or coal are unknown, one cannot exclude that oil inputs, industrial coal  
429 and/or fly ashes could contribute to the Pt enrichment at this sampling site given the range of  
430 values reported in the literature. Since 1953, a steel mill has also been present in the western  
431 area and related activities cause the release of particulate matter of different sizes (Mazzei et  
432 al., 2006). Metallurgic activities can be a source of Pt release into aquatic environments as  
433 recorded in other systems (e.g. Gironde fluvial estuarine continuum; Abdou et al., 2016).  
434 Furthermore, in urban systems, other possible Pt sources may arise from direct inputs of dental  
435 laboratories, electronic industries, glass manufacturing, Pt-containing pharmaceuticals or  
436 industrial catalyst productions (Kümmerer et al., 1999).

437

#### 438 *Hospital and sewage effluents*

439 Platinum-based compounds have been successfully applied in anti-cancer chemotherapy for  
440 decades (e.g. Lenz et al., 2007). Surface waters draining effluents from hospital with oncology  
441 ward contain patient excretion of Pt-based anticancer drugs and display Pt concentrations that  
442 could exceed natural inputs (Vyas et al., 2014). Monteiro et al. (2017) evaluated  $Pt_D$   
443 concentrations in the inflow and outflow of a wastewater treatment plant (WWTP) in Lisbon to  
444  $\sim 5$  and  $15 \text{ ng.L}^{-1}$  respectively after a dry weather period and  $\sim 10$  and  $25 \text{ ng.L}^{-1}$  after a raining  
445 event. In the western part of the Genoa Harbor, Pt inputs from sewage treatment plants reach  
446 the Polcevera river mouth (Fig. 1). Despite probable dilution in natural waters compared to  
447 levels previously reported, such inputs may add to Pt sources affecting the sampling site W3  
448 ( $Pt_D \sim 0.18 \text{ ng.L}^{-1}$ ). Small sewage effluents also occur directly in the Old Port (Fig. 1).  
449 Considering only the sites E1 to E4 located inside the relatively stagnant harbor waterbody (due  
450 to confinement and low tidal amplitudes; Cutroneo et al., 2017, 2012), the eastward gradients  
451 of Pt concentrations have been correlated with parameters reflecting sewage effluent signature.

452 Inside the harbor,  $Pt_D$  concentrations were positively correlated with dissolved oxygen ( $r > 0.9$ )  
453 and pH ( $r > 0.6$ ), and negatively correlated with turbidity, Chl-a, % POC, DOC, and  $NH_4^+$   
454 ( $r < -0.9$ ). The opposite trends occurred for  $Pt_P$  concentrations, which were positively correlated  
455 with Chl-a, % POC, DOC, and  $NH_4^+$ . Assuming that these major variables serve as proxies for  
456 wastewater inputs and degradation (Ruggieri et al., 2011), this could explain Pt distribution  
457 inside the Old Port. Accordingly, supply of discharged sewage rich in organic matter and poor  
458 in oxygen content typically occur into the harbor basins (Ruggieri et al., 2011). The CNR  
459 platform (site PF) and surrounding waters are close to the urban area hosting a relevant center  
460 for Medical Oncology (red cross/blue circle). Highest levels of  $Pt_P$  ( $14 \text{ ng.g}^{-1}$ ) are recorded at  
461 this sampling site and relatively higher levels of  $Pt_D$  ( $0.15 \text{ ng.L}^{-1}$ ) both at 12 pm. For the same  
462 sample, sewage-related signals are recorded, with clearly lower  $O_2$  saturation and highest POC  
463 levels compared to the other sites. Sites E1 and PF are also characterized by a more confined  
464 area with shallower bottom depth ( $\sim 6 \text{ m}$  depth). High levels of  $Pt_P$  and relatively low levels of  
465  $Pt_D$ , where sewage inputs are at maximum (site E1) might be related to: (i) the presence of  
466 originally high  $Pt_P$  concentrations in wastewaters or run-off, and/or (ii) the adsorption of  $Pt_D$  on  
467 organic-rich ligands present in wastewaters (high concentrations of dissolved and particulate  
468 organic carbon in the turbid sewage plume). The effect of sediment resuspension in these  
469 shallower sampling sites is not discarded. Kinetics of suspected adsorption/desorption  
470 processes may explain the observed differences in  $Pt_D$  and  $Pt_P$  distributions between sites (see  
471 *Section 4.3.*).

472

#### 473 *Traffic-related emissions*

474 The Genoa Harbor is in direct vicinity ( $< 5 \text{ km}$  distance) from the urban highway and very close  
475 to urban heavy traffic roads, a likely source for Pt bearing particles. Automobile catalysts,  
476 which are thought to be the principal Pt anthropogenic source, have atmospheric residence times

477 ranging from hours to days depending on particle size and density and can be transported from  
478 regional to longer distances (Rauch et al., 2006, 2004). Dust and suspended matter with Pt  
479 particles are thereafter removed from the atmosphere by wet (rainfall) or dry (gravitation)  
480 deposition (Pawlak et al., 2014). For other trace metals such as copper (Cu), enhanced  
481 atmospheric input of Cu-rich urban particles showing great water solubility may result in the  
482 predominance of the atmospheric input of Cu over the river input (El Sayed et al., 1994).  
483 Therefore, in addition to causing water mixing, wind can be a vector of Pt into aquatic systems.  
484 The two wind situations observed during our study are typical of the Genoa area. Winds from  
485 the N-NE (0–30° N) and SE (135–150° N) are two of the most frequent wind situations in  
486 winter and summer, respectively (Cutroneo et al., 2012). Our field campaign took place in  
487 spring, a period of the year generally featuring the two situations. The eastward profile was  
488 sampled under relatively strong N-NE winds causing the currents in the entire harbor to flow  
489 outwards (Cutroneo et al., 2012). Relatively clear gradients of all monitored parameters can be  
490 explained by such conditions. Recent data confirm the importance of atmospheric deposition in  
491 Pt enrichment of oceanic surface waters (López-Sánchez et al., 2019). Automobile catalyst  
492 exhaust Pt inputs come from the land and Pt-bearing particles can be transported by the wind  
493 causing a gradient of  $Pt_P$  concentrations eastward. In the Genoa Harbor system, such particles  
494 could originate from catalyst exhaust fumes and/or industrial fly ashes. On the reverse, the  
495 westward profile was carried out under weaker, SE winds and showed less clear parameter  
496 variations. The E and SE winds generate a westward current forcing the surface harbor waters  
497 inside, while only in the bottom layer a weak outflow can occur (Cutroneo et al. 2017, 2012).  
498 However, due to the morphological complexity and the port structures jutting out in all  
499 directions, there is an extreme variability in the current direction in the port (Capello et al.,  
500 2010) and more data would be needed covering longer time-scales to confirm the present  
501 assumptions. If such source types influence Pt partitioning and its spatial distribution, they also

502 may affect Pt levels both in historical records (e.g. Abdou et al., 2019, 2016) and at short  
503 temporal scales as observed in site PF.

504

#### 505 4.3. Platinum reactivity and partitioning

##### 506 *Platinum seawater speciation*

507 Platinum concentrations in both dissolved and particulate phases are controlled by several  
508 factors implying various biogeochemical processes. Assuming that Pt originates from multiple  
509 potential point sources prevailing at different sites it is likely that Pt speciation differs from site  
510 to site. Organic forms might be represented by the three Pt-based drugs mainly used in the  
511 hospital: cisplatin, carboplatin and oxaliplatin along with their metabolites, while Pt emitted  
512 from vehicles or industrial activities may be under inorganic forms. Hospital effluents transport  
513 dissolved Pt ranging from  $< 10 \text{ ng.L}^{-1}$  to  $250 \text{ }\mu\text{g.L}^{-1}$  (Rauch and Peucker-Ehrenbrink, 2015;  
514 Vyas et al., 2014), mainly excreted from these anticancer drugs and/or derived metabolites.  
515 Such excretion also continues outside the hospital, as more and more patients go home directly  
516 after the treatment to the extent that the majority of Pt is emitted from outpatients at home (Lenz  
517 et al., 2007; Vyas et., 2014). The phase in which Pt species are released as well as the  
518 dissolved/particulate partitioning in sewage and the related removal efficiency in WWTPs  
519 remain widely unknown. Previous studies suppose that municipal and hospital effluents contain  
520 carboplatin (the most stable drug) as well as degradation products being the monoaquacisplatin  
521 and the diaquacisplatin, from anti-cancer drug administration (Lenz et al., 2007; Vyas et al.,  
522 2014). Recent work reports that the behavior of organic Pt species in recipient waters is  
523 governed by chloride ( $\text{Cl}^-$ ) concentrations with, for cisplatin, decreasing proportion of reactive  
524 species with increasing salinity (Curtis et al., 2010; Turner and Mascorda, 2015). Curtis et al.  
525 (2010) proved that environmental conditions favoring cisplatin retention and its adsorption on



526 particles are turbid waters of low chlorinity and long residence time. Dispersal is likely to occur  
527 in rapidly flushed waters under low turbidity conditions and high chlorinity. Our study site is  
528 characterized by high salinities that may limit cisplatin adsorption, but turbid plumes arriving  
529 from sewage effluents and long water and particle residence times inside the breakwaters may  
530 in turn favor such process. More investigation is needed under similar environmental  
531 conditions.

532 Both run-off and sewage also contain PGE-bearing catalytic converter fragments with intact  
533 PGE-load (Prichard and Fisher, 2012), which may undergo partial dissolution in contact with  
534 seawater. The few data on Pt speciation in seawater suggest that Pt(IV) is the most important  
535 oxidation state (Cobelo-García et al., 2013). Laboratory works showed that its inorganic  
536 equilibrium speciation is dominated by the stable  $\text{PtCl}_5(\text{OH})^{2-}$  complex (Gammons, 1996;  
537 Cobelo-García et al., 2014a). Laboratory and field observations report decreasing particulate-  
538 aqueous distribution coefficient for inorganic forms with increasing salinity (Cobelo-García et  
539 al., 2014, 2008; Turner, 2007), suggesting increasing Pt levels in the dissolved phase as  $\text{Cl}^-$   
540 concentrations increase. The observed eastward particulate/dissolved gradients suggest Pt  
541 dissolution from solid carrier phases, either road dust (Sebek et al., 2011) or small sewage  
542 particles, and subsequent dilution of  $\text{Pt}_D$  by seawater that would be favored by Pt-Cl complex  
543 formation.

544 *Potential carrier phases of Pt in sites with anthropogenic influence*

545 Given the above, one would expect inputs of different co-existing Pt forms from different  
546 overlapping sources into the marine environment with wastewater, run-off of the surrounding  
547 area and atmospheric deposition. Numerous discharges occur in the Genoa Harbor area,  
548 comprising release of unknown and potentially dangerous substances (Fig. 1) that may  
549 contribute to Pt contamination. A rough mass balance ( $Pt_D = Pt_P \times SPM \times 10^{-3}$ ) for the eastern  
550 profile inside the harbor suggests that Pt release from suspended particles would account for a  
551  $Pt_D$  addition of  $\sim 0.02 \text{ ng.L}^{-1}$ , whereas the observed  $Pt_D$  values increased by  $\sim 0.06 \text{ ng.L}^{-1}$ . The  
552 amount of Pt presumably transferred from the particulate to the dissolved phase is not  
553 contradictory to the field data but does not explain all the  $Pt_D$  addition observed, supporting the  
554 idea of additional  $Pt_D$  inputs through the different discharges (Fig. 1). Outside the breakwaters,  
555 biogeochemical equilibration processes and the resulting higher  $Pt_D$  would be masked by  
556 massive dilution with open Mediterranean water. Biogeochemical processes, inherent to  
557 anthropogenic discharges and the mixing of environmental waters can widely modify the  
558 original Pt phase. Previous work has shown that relatively high dissolved metal loads in  
559 wastewater inputs equilibrate in the recipient waters. Efficient adsorption on high complexation  
560 site particles induces profound changes in element partitioning between the dissolved and  
561 particulate phases (e.g. Deycard et al., 2014). Indeed, the residual POC in effluent wastewater  
562 mainly consists of reactive (degradable) organic matter, once exposed to natural microorganism  
563 communities in the receiving waterbody (Deycard et al., 2017). Such organic matter and  
564 especially that containing thiols and reduced sulfur groups, may strongly bind soft metals and  
565 potentially compete with inorganic ligands such as  $Cl^-$  from the recipient waters (Levard et al.,  
566 2013; Wood et al., 1990). Literature suggests that, considering cisplatin flocculation in natural  
567 water, complexation with specific organic ligands containing nitrogen or sulphur is likely (e.g.  
568 Curtis et al., 2010; Turner and Mascorda, 2015). This means that Pt partitioning between the

569 two phases might be partly influenced by interactions with POC from wastewater discharges  
570 when mixing with coastal waters, although the degree of surface complexation with organic  
571 matter remains unknown (Couceiro et al., 2007). Natural sediments may also contain POC and  
572 laboratory experiments have proven that Pt adsorption kinetics onto estuarine sediments is  
573 greatest for cohesive sediments with relatively high total carbon contents (Couceiro et al.,  
574 2007). Another experimental study showed that complexation with organic ligands can be  
575 critical to particle-water fractionation of Pt discharged into aquatic systems, removal from the  
576 dissolved phase being most favorable when entering a turbid watercourse (Turner et al., 2006).  
577 All of these observations seem in line with the reported highest  $Pt_P$  levels co-occurring with  
578 high turbidity sewage inputs in the Genoa Harbor (Tables 1 and 3; Fig. 2B). Depth profiles of  
579  $Pt_D$  concentrations in the Atlantic Ocean also showed a higher particle-reactivity or lower  
580 solubility of  $Pt_D$  with decreasing oxygen levels (López-Sánchez et al., 2019).

581 The related daily variations in  $K_D$  values at site PF (Table 3) suggest that the observed  $K_D$  might  
582 not describe equilibrium conditions. However, the average  $K_D$  values obtained for the Genoa  
583 Harbor ( $\sim 8 \times 10^3$ ) are consistent with values obtained for the seawater end-member of the  
584 Gironde Estuary ( $\sim 4 \times 10^3$ , Cobelo-García et al., 2014a), and the maximum  $K_D$  value recorded  
585 at the CNR Platform ( $\sim 1 \times 10^5$ ) is similar to those found in the seawater end-member of the  
586 Lérez Estuary (Cobelo-García et al., 2013). Outside the Old Port, but still inside the harbor, the  
587 growing influence of open seawater with a decrease in turbidity, as well as change in the nature  
588 of SPM surfaces (decrease in %POC) could explain low  $Pt_P$  concentrations (below detection  
589 limit), going along with increasing  $Pt_D$ . Considering possible wind effect and water column  
590 mixing, remobilization of Pt from particles through the degradation of organic matter and redox  
591 reactions (correlation of Pt levels with pH and Eh parameters; Table 2) seems to contribute to  
592  $Pt_D$  enrichment at those sampling sites, as observed elsewhere for Pt and other trace metals  
593 (Almécija et al., 2016; El Sayed et al., 1994). However, multiple solid phases other than solely

594 POC can also decrease Pt<sub>D</sub> concentrations. Inorganic mineral phases such as iron and  
595 manganese oxides may also be important Pt carrier phases (Colodner et al., 1992). In fact, those  
596 phases could be more important than organic material for the removal of cisplatin degradation  
597 products (Turner and Mascorda, 2015).

598 Whatever the dissolved or particulate phase transporting Pt, this element has proven to be  
599 bioavailable to marine organisms (e.g. Rauch et al., 1999). It is crucial to better understand Pt  
600 speciation and distribution, since the physical and chemical forms of this emerging contaminant  
601 are expected to considerably influence its biological availability. In fact, previous work on Pt  
602 toxicity in marine bivalves has shown strong accumulation and the onset of defense  
603 mechanisms, for exposure levels that might be reached in case of acute pollution, especially in  
604 semi-closed coastal systems (Abdou et al., 2018).

605

#### 606 4.4. Coastal anthropogenic contamination – Pt as a novel urban tracer

607 Although the geochemical cycles of Pt in coastal environments under high urban/industrial  
608 pressure are far from being fully understood (due to the limited number of data), our study,  
609 combined to already existing works, allows to draw perspectives for future research in this field.  
610 Assuming the dominance of Pt organic forms released by hospital effluents, monitoring of Pt  
611 concentrations may serve as a tracer for these effluents release and spreading in the environment  
612 together with other proxies commonly used such as POC% or nutrient levels. Main substances  
613 expected in effluents are the most stable anti-cancer compounds (including carboplatin) and  
614 degradation products from the different drugs (Lenz et al., 2007; Vyas et al., 2014). However,  
615 important behavior differences (reactivity, phase affinity, removal...) are observed among Pt-  
616 based drugs and their various degradation products (Turner and Mascorda, 2015). Such organic  
617 Pt sources need monitoring and characterization, especially considering the increasing cancer

618 incidence and the related increasing demand for chemotherapy treatment in developed countries  
619 (Johnson et al., 2008). Inorganic forms of Pt are assumed to dominate in catalytic converters  
620 emissions. High resolution monitoring of concentrations of those forms could therefore reflect  
621 atmospheric particle deposition and traffic-related urban contamination in coastal areas.  
622 Inorganic Pt forms may also reflect atmospheric contamination related to industrial activities  
623 including oil and coal-based industries. The lack of knowledge regarding Pt speciation is  
624 directly related to analytical challenges inherent to the ultra-trace environmental levels of this  
625 emerging metallic contaminant. Future work should focus on developing analytical techniques  
626 for routine Pt quantification in seawater for both dissolved and particulate phases including  
627 speciation analyses.

628 Spatial distribution of Pt concentrations in the Genoa Harbor showed disparities partly  
629 depending on urban source proximity, yet, temporal aspects also may be crucial. Dredging  
630 activities, daily cycles in traffic intensity, industrial emissions, and/or wastewater composition  
631 (Deycard et al., 2014; Mazzei et al., 2006; Kümmerer and Helmers, 1997), as well as wind  
632 conditions could lead to variable fluxes of Pt into the harbor waters explaining why  $Pt_P$  varied  
633 by a factor of  $\sim 5$  (i.e. from 3 to 14  $ng.g^{-1}$  at site PF) within few hours. Spatial and temporal  
634 variations in Pt levels inside the Genoa Harbor may therefore reflect both distance from the  
635 source and release dynamics of a wide range of different potential sources.

636 Platinum distribution therefore appears to vary according to urban pollution type, source and  
637 intensity, suggesting that this element can serve as an innovative and sensitive tracer of  
638 anthropogenic impact from multiple urban sources (traffic, sewage, hospital effluents). The  
639 present dataset suggests that such anthropogenic inputs supplied to rivers or directly in the  
640 harbor by urban and/or industrial wastewater discharges and by atmospheric deposition may  
641 represent important local Pt point sources to coastal waters. Platinum levels observed in the  
642 Genoa Harbor waters are far lower than concentrations measured in highly contaminated waters

643 including polluted rivers (up to  $\sim 7 \text{ ng.L}^{-1}$  in Tokyo Bay urban rivers; Obata et al., 2006) or  
644 even hospital effluents (up to  $250 \mu\text{g.L}^{-1}$ ; Lenz et al., 2007; Vyas et al., 2014). It remains unclear  
645 to what extent dilution of Pt concentrations by recipient seawater or the absence of rainy events  
646 during our sample collection could have resulted in relatively low Pt levels. Future research and  
647 field sampling should therefore consider sample collection both near pollution sources (i.e.  
648 rivers, urban discharges, sewage effluents) and in recipient coastal waters in order to perform  
649 relevant mass balance calculations. This should be done at high spatial as well as high temporal  
650 resolutions in order to fully understand Pt cycles in urban coastal environments.

## 651 **5. Conclusions**

652 With TCE increasing environmental release being a global concern, this work provides  
653 knowledge on the extent of Pt contamination and biogeochemical processes occurring in a  
654 representative urban coastal site. The first information on Pt distribution and reactivity of both  
655 dissolved and particulate phases in an industrialized and urbanized Mediterranean harbor is  
656 given. Measured concentrations for  $Pt_D$  ( $\sim 0.08$  to  $0.18$   $ng.L^{-1}$ ) and  $Pt_P$  ( $< 0.34$  to  $14$   $ng.g^{-1}$ )  
657 allowed proposing  $Pt_D \sim 0.08$   $ng.L^{-1}$  (as measured in the Ligurian Current and south from the  
658 Balearic Islands) as a first reference value for western Mediterranean surface seawater. There  
659 is a clear evidence of anthropogenic Pt contamination at all sites studied within the Genoa  
660 Harbor showing distinct concentration gradients. They are attributed to different overlapping  
661 local sources such as industry, run-off, hospital effluents, domestic wastewater as well as  
662 physical parameters such as wind and dust / catalyst particles atmospheric deposition. Gradients  
663 in both  $Pt_D$  and  $Pt_P$  as well as major variables attributed to input and degradation of urban  
664 sewage inside the relatively stagnant harbor waters reflect biogeochemical processes modifying  
665 the nature, surface properties and abundance of suspended particles, leading to profound  
666 changes in Pt partitioning and carrier phases. While quantification of Pt emitted from vehicle  
667 exhaust, supposedly under inorganic form, rise attention, organic forms may also be of major  
668 concern in urbanized coastal systems. Such mobilization of anthropogenic Pt can enhance its  
669 bioavailability, bio-uptake and induce adverse effects on marine organisms. The role of  
670 biogeochemical processes and responses from marine wildlife to contamination, including  
671 potential Pt complexation to biologically-derived organic ligands such as algae exudates, are  
672 still unknown and need further investigation. On the other hand, this study opens the perspective  
673 of using Pt as an innovative tracer of urban inputs that should be applied in other urbanized  
674 coastal areas of the Mediterranean Sea and worldwide.

675 **Acknowledgements**

676 This work has greatly benefited from the financial support by the FEDER Aquitaine-1999-  
677 Z0061, the COST Action TD1407, and the EU FP7 Ocean 2013.2 Project SCHeMA (Project-  
678 Grant Agreement 614002), which is gratefully acknowledged. Authors are also thankful for the  
679 help of the UNIGE-It Team, the DISTAV, and the RV/MASO crew for sampling and  
680 assistance. Analytical support from Dominique Poirier, Céline Charbonnier and Aude Charrier  
681 is greatly acknowledged.

682

683 **Conflicts of interest**

684 The authors declare no conflicts of interest.

685



686 **References**

- 687 Abdou, M., Schäfer, J., Cobelo-García, A., Neira, P., Petit, J.C.J., Auger, D., Chiffolleau, J.-F.,  
688 Blanc, G., 2016. Past and present platinum contamination of a major European fluvial–estuarine  
689 system: Insights from river sediments and estuarine oysters. *Marine Chemistry*, 13th  
690 International Estuarine Biogeochemistry Symposium (IEBS) - Estuaries Under Anthropogenic  
691 Pressure **185**, 104–110. <https://doi.org/10.1016/j.marchem.2016.01.006>
- 692 Abdou, M., Dutruch, L., Schäfer, J., Zaldibar, B., Medrano, R., Izagirre, U., Gil-Díaz, T., Bossy,  
693 C., Catrouillet, C., Hu, R., Coynel, A., Lerat, A., Cobelo-García, A., Blanc, G., Soto, M., 2018.  
694 Tracing platinum accumulation kinetics in oyster *Crassostrea gigas*, a sentinel species in  
695 coastal marine environments. *Science of the Total Environment* **615**, 652–663.  
696 <https://doi.org/10.1016/j.scitotenv.2017.09.078>
- 697 Abdou, M., Schäfer, J., Hu, R., Gil-Díaz, T., Garnier, C., Brach-Papa, C., Chiffolleau, J.-F.,  
698 Charmasson, S., Giner, F., Dutruch, L., Blanc, G., 2019. Platinum in sediments and mussels  
699 from the northwestern Mediterranean coast: Temporal and spatial aspects. *Chemosphere* **215**,  
700 783–792. <https://doi.org/10.1016/j.chemosphere.2018.10.011>
- 701 Aminot, A., Kirkwood, D.S., Kérouel, R., 1997. Determination of ammonia in seawater by the  
702 indophenol-blue method: Evaluation of the ICES NUTS I/C 5 questionnaire. *Marine Chemistry*  
703 **56**, 59–75. [https://doi.org/10.1016/S0304-4203\(96\)00080-1](https://doi.org/10.1016/S0304-4203(96)00080-1)
- 704 Capello, M., Cutroneo, L., Ferretti, G., Gallino, S., Canepa, G., 2016. Changes in the physical  
705 characteristics of the water column at the mouth of a torrent during an extreme rainfall event.  
706 *Journal of Hydrology, Flash floods, hydro-geomorphic response and risk management* **541**,  
707 146–157. <https://doi.org/10.1016/j.jhydrol.2015.12.009>
- 708 Capello, M., Cutroneo, L., Castellano, M., Orsi, M., Pieracci, A., Maria Bertolotto, R., Povero,  
709 P., Tucci, S., 2010. Physical and sedimentological characterisation of dredged sediments.  
710 *Chemistry and Ecology* **26**, 359–369. <https://doi.org/10.1080/02757541003627746>
- 711 Cobelo-García, A., Filella, M., Croot, P., Frazzoli, C., Du Laing, G., Ospina-Alvarez, N.,  
712 Rauch, S., Salaun, P., Schäfer, J., Zimmermann, S., 2015. COST action TD1407: network on  
713 technology-critical elements (NOTICE)--from environmental processes to human health  
714 threats. *Environmental Science Pollution Research* **22**, 15188–15194.  
715 <https://doi.org/10.1007/s11356-015-5221-0>
- 716 Cobelo-García, A., López-Sánchez, D.E., Almécija, C., Santos-Echeandía, J., 2013. Behavior  
717 of platinum during estuarine mixing (Pontevedra Ria, NW Iberian Peninsula). *Marine*  
718 *Chemistry* **150**, 11–18. <https://doi.org/10.1016/j.marchem.2013.01.005>
- 719 Cobelo-García, A., López-Sánchez, D.E., Schäfer, J., Petit, J.C.J., Blanc, G., Turner, A., 2014a.  
720 Behavior and fluxes of Pt in the macrotidal Gironde Estuary (SW France). *Marine Chemistry*  
721 **167**, 93–101. <https://doi.org/10.1016/j.marchem.2014.07.006>
- 722 Cobelo-García, A., Santos-Echeandía, J., López-Sánchez, D.E., Almécija, C., Omanović, D.,  
723 2014b. Improving the voltammetric quantification of ill-defined peaks using second derivative

724 signal transformation: Example of the determination of platinum in water and sediments.  
725 *Analytical Chemistry* **86**, 2308–2313. <https://doi.org/10.1021/ac403558y>

726 Cobelo-García, A., Turner, A., Millward, G.E., 2008. Fractionation and reactivity of platinum  
727 group elements during estuarine mixing. *Environmental Science & Technology* **42**, 1096–1101.  
728 <https://doi.org/10.1021/es0712118>

729 Colodner, D., 1991. The Marine Geochemistry of Rhenium, Iridium and Platinum. PhD Thesis,  
730 Massachusetts Institute of Technology, USA.

731 Colodner, D.C., Boyle, E.A., Edmond, J.M., Thomson, J., 1992. Post-depositional mobility of  
732 platinum, iridium and rhenium in marine sediments. *Nature* **358**, 402–404.  
733 <https://doi.org/10.1038/358402a0>

734 Couceiro, F., Turner, A., Millward, G.E., 2007. Adsorption and desorption kinetics of rhodium  
735 (III) and platinum (IV) in turbid suspensions: Potential tracers for sediment transport in  
736 estuarine flumes. *Marine Chemistry*, 9th International Estuarine Biogeochemistry Symposium  
737 Estuaries and Enclosed Seas under Changing Environmental Conditions **107**, 308–318.  
738 <https://doi.org/10.1016/j.marchem.2007.02.010>

739 Curtis, L., Turner, A., Vyas, N., Sewell, G., 2010. Speciation and Reactivity of Cisplatin in  
740 River Water and Seawater. *Environ. Sci. Technol.* **44**, 3345–3350.  
741 <https://doi.org/10.1021/es903620z>

742 Cutroneo, L., Castellano, M., Pieracci, A., Povero, P., Tucci, S., Capello, M., 2012. The use of  
743 a combined monitoring system for following a turbid plume generated by dredging activities in  
744 a port. *Journal of Soils and Sediments* **12**, 797–809. [https://doi.org/10.1007/s11368-012-0486-](https://doi.org/10.1007/s11368-012-0486-0)  
745 [0](https://doi.org/10.1007/s11368-012-0486-0)

746 Cutroneo, L., Carbone, C., Consani, S., Vagge, G., Canepa, G., Capello, M., 2017.  
747 Environmental complexity of a port: Evidence from circulation of the water masses, and  
748 composition and contamination of bottom sediments. *Marine Pollution Bulletin* **119**, 184–194.  
749 <https://doi.org/10.1016/j.marpolbul.2017.03.058>

750 Dai, S., Ren, D., Zhang, J., Hou, X., 2003. Concentrations and origins of platinum group  
751 elements in Late Paleozoic coals of China. *International Journal of Coal Geology* **55**, 59–70.  
752 [https://doi.org/10.1016/S0166-5162\(03\)00079-X](https://doi.org/10.1016/S0166-5162(03)00079-X)

753 Deycard, V.N., Schäfer, J., Blanc, G., Coynel, A., Petit, J.C.J., Lancelleur, L., Dutruch, L.,  
754 Bossy, C., Ventura, A., 2014. Contributions and potential impacts of seven priority substances  
755 (As, Cd, Cu, Cr, Ni, Pb, and Zn) to a major European Estuary (Gironde Estuary, France) from  
756 urban wastewater. *Marine Chemistry*, Estuarine Biogeochemistry **167**, 123–134.  
757 <https://doi.org/10.1016/j.marchem.2014.05.005>

758 Deycard, V.N., Schäfer, J., Petit, J.C.J., Coynel, A., Lancelleur, L., Dutruch, L., Bossy, C.,  
759 Ventura, A., Blanc, G., 2017. Inputs, dynamics and potential impacts of silver (Ag) from urban  
760 wastewater to a highly turbid estuary (SW France). *Chemosphere* **167**, 501–511.  
761 <https://doi.org/10.1016/j.chemosphere.2016.09.154>

- 762 Djingova, R., Heidenreich, H., Kovacheva, P., Markert, B., 2003. On the determination of  
763 platinum group elements in environmental materials by inductively coupled plasma mass  
764 spectrometry and microwave digestion. *Analytica Chimica Acta* **489**, 245–251.  
765 [https://doi.org/10.1016/S0003-2670\(03\)00716-5](https://doi.org/10.1016/S0003-2670(03)00716-5)
- 766 El Sayed, M.A., Aminot, A., Kerouel, R., 1994. Nutrients and trace metals in the northwestern  
767 Mediterranean under coastal upwelling conditions. *Continental Shelf Research* **14**, 507–530.  
768 [https://doi.org/10.1016/0278-4343\(94\)90101-5](https://doi.org/10.1016/0278-4343(94)90101-5)
- 769 Finkelman, R.B., Aruscavage, P.J., 1981. Concentration of some platinum-group metals in coal.  
770 *International Journal of Coal Geology* **1**, 95–99. [https://doi.org/10.1016/0166-5162\(81\)90006-](https://doi.org/10.1016/0166-5162(81)90006-9)  
771 [9](https://doi.org/10.1016/0166-5162(81)90006-9)
- 772 Gammons, C.H., 1996. Experimental investigations of the hydrothermal geochemistry of  
773 platinum and palladium: V. Equilibria between platinum metal, Pt(II), and Pt(IV) chloride  
774 complexes at 25 to 300°C. *Geochimica et Cosmochimica Acta* **60**, 1683–1694.  
775 [https://doi.org/10.1016/0016-7037\(96\)00048-8](https://doi.org/10.1016/0016-7037(96)00048-8)
- 776 Goldberg, E.D., Hodge, V., Kay, P., Stallard, M., Koide, M., 1986. Some comparative marine  
777 chemistries of platinum and iridium. *Applied Geochemistry* **1**, 227–232.  
778 [https://doi.org/10.1016/0883-2927\(86\)90006-5](https://doi.org/10.1016/0883-2927(86)90006-5)
- 779 Johnson, A.C., Jürgens, M.D., Williams, R.J., Kümmerer, K., Kortenkamp, A., Sumpter, J.P.,  
780 2008. Do cytotoxic chemotherapy drugs discharged into rivers pose a risk to the environment  
781 and human health? An overview and UK case study. *Journal of Hydrology* **348**, 167–175.  
782 <https://doi.org/10.1016/j.jhydrol.2007.09.054>
- 783 Kümmerer, K., Helters, E., 1997. Hospital effluents as a source for platinum in the  
784 environment. *Science of the Total Environment* **193**, 179–184. [https://doi.org/10.1016/S0048-](https://doi.org/10.1016/S0048-9697(96)05331-4)  
785 [9697\(96\)05331-4](https://doi.org/10.1016/S0048-9697(96)05331-4)
- 786 Kümmerer K, Helters E, Hubner P, Mascart G, Milandri M, Reinthaler F, Zwakenberg M  
787 (1999) European hospitals as a source for platinum in the environment in comparison with other  
788 sources. *Science of the Total Environment* **225**:155–165. [https://doi.org/10.1016/S0048-](https://doi.org/10.1016/S0048-9697(98)00341-6)  
789 [9697\(98\)00341-6](https://doi.org/10.1016/S0048-9697(98)00341-6)
- 790 Lenz, K., Koellensperger, G., Hann, S., Weissenbacher, N., Mahnik, S.N., Fuerhacker, M.,  
791 2007. Fate of cancerostatic platinum compounds in biological wastewater treatment of hospital  
792 effluents. *Chemosphere* **69**, 1765–1774. <https://doi.org/10.1016/j.chemosphere.2007.05.062>
- 793 Levard, C., Mitra, S., Yang, T., Jew, A.D., Badireddy, A.R., Lowry, G.V., Brown, G.E., 2013.  
794 Effect of Chloride on the Dissolution Rate of Silver Nanoparticles and Toxicity to *E. coli*.  
795 *Environmental Science & Technology* **47**, 5738–5745. <https://doi.org/10.1021/es400396f>
- 796 López-Sánchez, D.E., Cobelo-García, A., Rijkenberg, M.J.A., Gerringa, L.J.A., de Baar,  
797 H.J.W., 2019. New insights on the dissolved platinum behavior in the Atlantic Ocean. *Chemical*  
798 *Geology* **511**, 204–211. <https://doi.org/10.1016/j.chemgeo.2019.01.003>

799 Martín, J., Sanchez-Cabeza, J.A., Eriksson, M., Levy, I., Miquel, J.C., 2009. Recent  
800 accumulation of trace metals in sediments at the DYFAMED site (Northwestern Mediterranean  
801 Sea). *Marine Pollution Bulletin*, Environmental Records of Anthropogenic Impacts on Coastal  
802 Ecosystems **59**, 146–153. <https://doi.org/10.1016/j.marpolbul.2009.03.013>

803 Mashio, A.S., Obata, H., Gamo, T., 2017. Dissolved Platinum Concentrations in Coastal  
804 Seawater: Boso to Sanriku Areas, Japan. *Archives of Environmental Contamination and*  
805 *Toxicology* **73**, 240–246. <https://doi.org/10.1007/s00244-017-0373-1>

806 Mashio, A.S., Obata, H., Tazoe, H., Tsutsumi, M., Ferrer i Santos, A., Gamo, T., 2016.  
807 Dissolved platinum in rainwater, river water and seawater around Tokyo Bay and Otsuchi Bay  
808 in Japan. *Estuarine Coastal Shelf Science* **180**, 160–167.  
809 <https://doi.org/10.1016/j.ecss.2016.07.002>

810 Mazzei, F., D’Alessandro, A., Lucarelli, F., Marengo, F., Nava, S., Prati, P., Valli, G., Vecchi,  
811 R., 2006. Elemental composition and source apportionment of particulate matter near a steel  
812 plant in Genoa (Italy). *Nuclear Instruments and Methods in Physics Research Section B: Beam*  
813 *Interactions with Materials and Atoms*, Ion Beam Analysis **249**, 548–551.  
814 <https://doi.org/10.1016/j.nimb.2006.03.050>

815 Monteiro, C.E., Cobelo-García, A., Caetano, M., Correia dos Santos, M.M., 2017. Improved  
816 voltammetric method for simultaneous determination of Pt and Rh using second derivative  
817 signal transformation – application to environmental samples. *Talanta* **175**, 1–8.  
818 <https://doi.org/10.1016/j.talanta.2017.06.067>

819 Neira, P., Cobelo-García, A., Besada, V., Santos-Echeandía, J., Bellas, J., 2015. Evidence of  
820 increased anthropogenic emissions of platinum: Time-series analysis of mussels (1991-2011)  
821 of an urban beach. *Science of the Total Environment* **514C**, 366–370.  
822 <https://doi.org/10.1016/j.scitotenv.2015.02.016>

823 Obata, H., Yoshida, T., Ogawa, H., 2006. Determination of picomolar levels of platinum in  
824 estuarine waters: A comparison of cathodic stripping voltammetry and isotope dilution-  
825 inductively coupled plasma mass spectrometry. *Analytica Chimica Acta* **580**, 32–38.  
826 <https://doi.org/10.1016/j.aca.2006.07.044>

827 Oursel, B., Garnier, C., Durrieu, G., Mounier, S., Omanović, D., Lucas, Y., 2013. Dynamics  
828 and fates of trace metals chronically input in a Mediterranean coastal zone impacted by a large  
829 urban area. *Marine Pollution Bulletin* **69**, 137–149.  
830 <https://doi.org/10.1016/j.marpolbul.2013.01.023>

831 Pawlak, J., Lodyga-Chruścińska, E., Chrustowicz, J., 2014. Fate of platinum metals in the  
832 environment. *Journal of Trace Elements in Medicine and Biology* **28**, 247–254.  
833 <https://doi.org/10.1016/j.jtemb.2014.03.005>

834 Peavy, C.C., 1958. The importance of platinum in petroleum refining. *Johns. Matthey Technol.*  
835 *Rev., Platinum Metals Review* **48**, 5.

836 Povero, P., Ruggieri, N., Misic, C., Castellano, M., Rivaro, P., Conio, O., Derqui, E., Maggi,  
837 S., Fabiano, M. 2005. Ports of Genoa: Old Port, Multedo Oil Terminal and Voltri Container

838 Terminal. In: Nutrient fluxes in transition zones of the Italian Coast. Giordani G., P. Viaroli, D.  
839 P. Swaney, C. N. Murray, J. M. Zaldivar and J. J. Marshall Crossland (eds). *Loicz Reports &*  
840 *Studies* **28**.

841 Pougnet, F., Schäfer, J., Dutruch, L., Garnier, C., Tessier, E., Dang, H., Lancelleur, L., Mullot,  
842 J. ulrich, Lenoble, V., Blanc, G., 2014. Sources and historical record of tin and butyl-tin species  
843 in a Mediterranean bay (Toulon Bay, France). *Environmental Science and Pollution Research*  
844 **21**, 6640–6651. <https://doi.org/10.1007/s11356-014-2576-6>

845 Prichard, H.M., Fisher, P.C., 2012. Identification of Platinum and Palladium Particles Emitted  
846 from Vehicles and Dispersed into the Surface Environment. *Environmental Science &*  
847 *Technology* **46**, 3149–3154. <https://doi.org/10.1021/es203666h>

848 Rauch, S., F. Hemond, H., Peucker-Ehrenbrink, B., 2004. Source characterisation of  
849 atmospheric platinum group element deposition into an ombrotrophic peat bog. *Journal of*  
850 *Environmental Monitoring* **6**, 335–343. <https://doi.org/10.1039/B316547G>

851 Rauch, S., Morrison, G.M., 1999. Platinum uptake by the freshwater isopod *Asellus aquaticus*  
852 in urban rivers. *Science of the Total Environment* **235**, 261–268. [https://doi.org/10.1016/S0048-](https://doi.org/10.1016/S0048-9697(99)00203-X)  
853 [9697\(99\)00203-X](https://doi.org/10.1016/S0048-9697(99)00203-X)

854 Rauch, S., Peucker-Ehrenbrink, B., 2015. Sources of Platinum Group Elements in the  
855 Environment, in: Platinum Metals in the Environment, *Environmental Science and*  
856 *Engineering*. Springer, Berlin, Heidelberg, pp. 3–17. [https://doi.org/10.1007/978-3-662-44559-](https://doi.org/10.1007/978-3-662-44559-4_1)  
857 [4\\_1](https://doi.org/10.1007/978-3-662-44559-4_1)

858 Rauch, S., Peucker-Ehrenbrink, B., Molina, L.T., Molina, M.J., Ramos, R., Hemond, H.F.,  
859 2006. Platinum Group Elements in Airborne Particles in Mexico City. *Environmental Science*  
860 *& Technology* **40**, 7554–7560. <https://doi.org/10.1021/es061470h>

861 Recchia, V., 1999. Risk Communication and Public Perception of Technological Hazards (Part  
862 Two) (SSRN Scholarly Paper No. ID 200570). Social Science Research Network, Rochester,  
863 NY

864 Rudnick, R.L., Gao, S., 2003. Composition of the Continental Crust, in: *Treatise on*  
865 *Geochemistry*. Elsevier, pp. 1–64.

866 Ruggieri, N., Castellano, M., Capello, M., Maggi, S., Povero, P., 2011. Seasonal and spatial  
867 variability of water quality parameters in the Port of Genoa, Italy, from 2000 to 2007. *Marine*  
868 *Pollution Bulletin* **62**, 340–349. <https://doi.org/10.1016/j.marpolbul.2010.10.006>

869 Schäfer, J., Blanc, G., Lapaquellerie, Y., Maillet, N., Maneux, E., Etcheber, H., 2002. Ten-year  
870 observation of the Gironde tributary fluvial system: Fluxes of suspended matter, particulate  
871 organic carbon and cadmium. *Marine Chemistry* **79**, 229–242. [https://doi.org/10.1016/S0304-](https://doi.org/10.1016/S0304-4203(02)00066-X)  
872 [4203\(02\)00066-X](https://doi.org/10.1016/S0304-4203(02)00066-X)

873 Schäfer, J., Eckhardt, J.-D., Berner, Z.A., Stüben, D., 1999. Time-Dependent Increase of  
874 Traffic-Emitted Platinum-Group Elements (PGE) in Different Environmental Compartments.  
875 *Environmental Science & Technology* **33**, 3166–3170. <https://doi.org/10.1021/es990033i>

876 Sebek, O., Mihaljevič, M., Strnad, L., Ettler, V., Ježek, J., Stědrý, R., Drahota, P., Ackerman,  
877 L., Adamec, V., 2011. Dissolution kinetics of Pd and Pt from automobile catalysts by naturally  
878 occurring complexing agents. *Journal of Hazardous Materials* **198**, 331–339.  
879 <https://doi.org/10.1016/j.jhazmat.2011.10.051>

880 Sharp, J.H., Benner, R., Bennett, L., Carlson, C.A., Dow, R., Fitzwater, S.E., 1993. Re-  
881 evaluation of high temperature combustion and chemical oxidation measurements of dissolved  
882 organic carbon in seawater. *Limnology and Oceanography* **38**, 1774–1782.  
883 <https://doi.org/10.4319/lo.1993.38.8.1774>

884 Small, C., Nicholls, R.J., 2003. A global analysis of human settlement in coastal zones. *Journal*  
885 *of Coastal Research* **19**, 584–599.

886 Suzuki, A., Obata, H., Okubo, A., Gamo, T., 2014. Precise determination of dissolved platinum  
887 in seawater of the Japan Sea, Sea of Okhotsk and western North Pacific Ocean. *Marine*  
888 *Chemistry* **166**, 114–121. <https://doi.org/10.1016/j.marchem.2014.10.003>

889 Tessier, E., Garnier, C., Mullot, J.-U., Lenoble, V., Arnaud, M., Raynaud, M., Mounier, S.,  
890 2011. Study of the spatial and historical distribution of sediment inorganic contamination in the  
891 Toulon bay (France). *Marine Pollution Bulletin* **62**, 2075–2086.  
892 <https://doi.org/10.1016/j.marpolbul.2011.07.022>

893 Turetta, C., Cozzi, G., Varga, A., Barbante, C., Capodaglio, G., Cescon, P., 2003. Platinum  
894 group elements determination in seawater by ICP-SFMS: Initial results. *J. Phys. IV France* **107**,  
895 1321–1324. <https://doi.org/10.1051/jp4:20030544>

896 Turner, A., Mascorda, L., 2015. Particle–water interactions of platinum-based anticancer drugs  
897 in river water and estuarine water. *Chemosphere* **119**, 415–422.  
898 <https://doi.org/10.1016/j.chemosphere.2014.06.074>

899 Turner, A., 2007. Particle–water interactions of platinum group elements under estuarine  
900 conditions. *Marine Chemistry* **103**, 103–111. <https://doi.org/10.1016/j.marchem.2006.08.002>

901 Turner, A., Crussell, M., Millward, G.E., Cobelo-García, A., Fisher, A.S., 2006. Adsorption  
902 Kinetics of Platinum Group Elements in River Water. *Environmental Science & Technology*  
903 **40**, 1524–1531. <https://doi.org/10.1021/es0518124>

904 van den Berg, C.M.G., Jacinto, G.S., 1988. The determination of platinum in sea water by  
905 adsorptive cathodic stripping voltammetry. *Analytica Chimica Acta* **211**, 129–139.

906 Vyas, N., Turner, A., Sewell, G., 2014. Platinum-based anticancer drugs in waste waters of a  
907 major UK hospital and predicted concentrations in recipient surface waters. *Science of the Total*  
908 *Environment* **493**, 324–329. <https://doi.org/10.1016/j.scitotenv.2014.05.127>

909 Wood, S.A., 1990. The interaction of dissolved platinum with fulvic acid and simple organic  
910 acid analogues in aqueous solutions. *Canadian Mineralogist* **28**, 665–673.

911

912 **Tables**

913 **Table 1:** Dissolved and particulate Pt concentrations, Pt distribution coefficients, and master  
 914 variables monitored along two longitudinal profiles in the Genoa Harbor. The eastward profile  
 915 corresponds to sites E1 to E6, with E1 being located in the Old Port, while the westward profile  
 916 corresponds to sites W1 to W6. With: Dissolved Pt concentration ( $Pt_D$ ;  $ng.L^{-1}$ ), Particulate Pt  
 917 concentration ( $Pt_P$ ;  $ng.g^{-1}$ ), Particle-water distribution coefficient ( $K_D$ ), Wind direction (Wind  
 918 dir.), Wind speed (Wind sp.;  $km.h^{-1}$ ), Bottom depth (m), Turbidity (Turb.; NTU), Temperature  
 919 (Temp;  $^{\circ}C$ ), Salinity, Redox potential (Eh; mV), pH, dissolved oxygen saturation ( $O_2\%$ ),  
 920 Dissolved Organic Carbon (DOC; mg/L), Particulate Organic Carbon (POC%), Chlorophyll-a  
 921 (Chl-a;  $\mu g/L$ ), ammonium ( $NH_4^+$ ;  $\mu g/L$ ), d.l.: detection limits, n.d.: not determined.

Param./Site	W6	W5	W4	W3	W2	W1	E1	E2	E3	E4	E5	E6
<b><math>Pt_D</math></b>	0.10	0.11	0.14	0.17	0.16	0.17	0.12	0.15	0.15	0.18	0.08	0.08
<b><math>Pt_P</math></b>	<d.l.	0.99	<d.l.	0.65	0.65	0.37	2.6	1.4	<d.l.	0.50	<d.l.	<d.l.
<b><math>K_D</math> (<math>\times 10^3</math>)</b>	n.d.	9.1	n.d.	3.7	4.1	2.2	23	9.9	n.d.	2.8	n.d.	n.d.
<b>Wind dir.</b>	ESE	SSE	SSE	SE	S	SSE	N	NNE	N	NE	N	N
<b>Wind sp.</b>	15	9	7	9	6	6	7	17	22	15	22	15
<b>Bottom depth</b>	24.3	27.6	11.0	13.0	11.0	9.6	6.0	9.7	10.7	16.0	12.5	15.0
<b>Turb.</b>	2.23	7.38	2.89	5.17	2.51	4.17	6.47	4.85	3.88	3.52	2.10	2.13
<b>Temp.</b>	14.61	14.82	14.88	14.80	14.84	15.02	14.94	14.84	14.85	14.96	14.50	14.88
<b>Salinity</b>	38.0	37.9	38.0	38.0	38.0	37.8	37.8	37.7	37.8	37.8	38.1	38.0
<b>Eh</b>	204	203	168	187	187	179	173	182	196	211	181	196
<b>pH</b>	8.24	8.21	8.17	8.22	8.22	8.18	8.14	8.14	8.19	8.17	8.21	8.20
<b><math>O_2\%</math></b>	94.5	92.5	93.9	90.4	96.0	92.6	69.1	87.9	91.4	94.0	97.9	96.8
<b>DOC</b>	1.05	1.17	1.16	0.98	0.84	1.14	2.05	1.28	1.10	0.68	0.91	1.04
<b>POC%</b>	3.75	2.81	2.60	4.87	2.32	0.89	4.81	2.73	3.11	2.47	4.35	1.94
<b>Chl-a</b>	0.37	1.02	1.12	1.48	0.59	0.95	1.16	0.98	0.82	0.82	0.25	0.35
<b><math>NH_4^+</math></b>	<d.l.	25.1	<d.l.	41.5	<d.l.	<d.l.	137	113	111	102	<d.l.	<d.l.

922

923 **Table 2:** Correlation table of  $Pt_D$  and  $Pt_P$  concentrations with master variables. Values correspond to  
 924 Pearson's  $r$  coefficient. n.d.: not determined. Stars correspond to a significant level of 0.05 ( $p$ -  
 925 value<0.05). Note that only the sites inside the breakwaters are considered.

	Eastward profile (E1 to E4)		Westward profile (W1 to W4)	
	$Pt_D$	$Pt_P$	$Pt_D$	$Pt_P$
Wind sp.	0.59	-0.90	0.43	0.52
Turb.	-0.95*	1.00*	0.80	-0.12
Temp.	0.15	-0.14	-0.07	-0.99*
Salinity	0.43	-0.34	-0.39	0.99*
Eh	0.96*	-0.93	0.83	1.00*
pH	0.63	-0.86	0.63	1.00*
O <sub>2</sub> %	0.92*	-0.98*	-0.62	0.10
DOC	-0.99*	1.00*	-0.35	-0.87
POC%	-0.90*	0.94	0.36	0.79
Chl-a	-0.91*	1.00*	0.33	0.12
NH <sub>4</sub> <sup>+</sup>	-0.97*	0.99*	n.d.	n.d.

926

927 **Table 3:** Dissolved and particulate Pt concentrations, particle-water distribution coefficients,  
 928 and master variables at the CNR Platform (site PF) at 10 am, 12 pm, and 2 pm. Units of the  
 929 various parameters are as reported in Table 1.

Param./Time	10 am	12 pm	2 pm
$Pt_D$	0.09	0.15	0.11
$Pt_P$	7.7	14	3.1
$K_D$ ( $\times 10^3$ )	82	94	27
Wind dir.	N	SSE	S
Wind sp.	4	9	7
Bottom depth	6	6	6
Turb.	4.00	2.60	4.60
Temp.	14.76	14.66	14.73
Salinity	38.0	38.0	38.0
Eh	190	182	191
pH	8.20	8.20	8.21
O <sub>2</sub> %	81.9	82.8	87.1
DOC	1.01	0.68	0.63
POC%	2.50	5.15	2.02
Chl-a	1.00	1.40	1.60
NH <sub>4</sub> <sup>+</sup>	47.0	48.1	44.8

930



931 **Figure captions**

932 **Fig. 1:** Sampling sites in the Genoa Harbor. Two sampling profiles were performed with an  
933 eastward profile (sites E1 to E6) and a westward profile (sites W1 to W6). Sampling site PF  
934 (PlatForm) corresponds to the CNR Platform. White arrows indicate river mouths. WWTPs:  
935 Wastewater Treatment Plants.

936 **Fig. 2:** Dissolved and particulate Pt concentrations along the two longitudinal profiles in the  
937 Genoa Harbor. A: spatial distribution of dissolved Pt concentrations ( $Pt_D$ ;  $ng.L^{-1}$ ); and B: spatial  
938 distribution of particulate Pt concentrations ( $Pt_P$ ;  $ng.g^{-1}$ ).

939

940 **List of tables:**

941 **Table 1:** Dissolved and particulate Pt concentrations, Pt distribution coefficients, and master  
942 variables monitored along two longitudinal profiles in the Genoa Harbor. The eastward profile  
943 corresponds to sites E1 to E6, with E1 being located in the Old Port, while the westward profile  
944 corresponds to sites W1 to W6. With: Dissolved Pt concentration ( $Pt_D$ ;  $ng.L^{-1}$ ), Particulate Pt  
945 concentration ( $Pt_P$ ;  $ng.g^{-1}$ ), Particle-water distribution coefficient ( $K_D$ ), Wind direction (Wind  
946 dir.), Wind speed (Wind sp.;  $km.h^{-1}$ ), Bottom depth (m), Turbidity (Turb.; NTU), Temperature  
947 (Temp;  $^{\circ}C$ ), Salinity, Redox potential (Eh; mV), pH, dissolved oxygen saturation ( $O_2\%$ ),  
948 Dissolved Organic Carbon (DOC; mg/L), Particulate Organic Carbon (POC%), Chlorophyll-a  
949 (Chl-a;  $\mu g/L$ ), ammonium ( $NH_4^+$ ;  $\mu g/L$ ), d.l.: detection limits, n.d.: not determined.

950 **Table 2:** Correlation table of  $Pt_D$  and  $Pt_P$  concentrations with master variables. Values  
951 correspond to Pearson's r coefficient. n.d.: not determined. Stars correspond to a significant  
952 level of 0.05 ( $p\text{-value}<0.05$ ). Note that only the sites inside the breakwaterss are considered.

953 **Table 3:** Dissolved and particulate Pt concentrations, particle-water distribution coefficients,  
954 and master variables at the CNR Platform (site PF) at 10 am, 12 pm, and 2 pm. Turb.: turbidity.  
955 Units of the various parameters are as reported in Table 1.